Inorg. Chem. **2009**, *48*, 231−238

Flash and Continuous Photolysis Studies of the Thionitrosyl Complex $Cr(CH_3CN)_5(NS)^{2+}$ and the Nitric Oxide Analogs: Reactions of Nitrogen Monosulfide in Solution

Johannes W. Dethlefsen,[†] Erik D. Hedegård,[†] R. Dale Rimmer,[‡] Peter C. Ford,*[,‡] and Anders Døssing*[,†]

Department of Chemistry, University of Copenhagen, Universitetsparken 5, DK-2100 Copenhagen Ø, Denmark, and Department of Chemistry and Biochemistry, University of California, Santa Barbara, Santa Barbara, California 93106-9510

Received September 3, 2008

Photolysis of the thionitrosyl complex $Cr(CH_3CN)_5(NS)^{2+}$ (**1**) in acetonitrile solution leads to the dissociation of nitrogen monosulfide (NS). In deaerated solution, this reaction is reversible, and flash photolysis studies demonstrate that NS reacts with $Cr(CH_3CN)_6^{2+}$ according to the rate law $d[\mathbf{1}]/dt = k_{on}[Cr(CH_3CN)_6^{2+}][NS]$ ($k_{on} = 2.3 \times 10^8$ M^{-1} s^{-1} at 298 K). The photolysis of **1** in deaerated acetonitrile with added $Fe(S_2CNEt_2)_2$ leads to the transfer of NS and the formation of a species concluded to be $Fe(S_2CNEt_2)_2(NS)$ based on its electron paramagnetic resonance spectrum. Analogous photolysis of **1** in the presence of added NO leads to clean formation of the nitrosyl complex $Cr(CH_3CN)_5(NO)^{2+}$ (**2**) presumably by NO capture of the photoproduct $Cr(CH_3CN)_6^{2+}$ (**3**). When **1** was photolyzed in aerated acetonitrile solution, the reactive species **3** was trapped, thus leading to net photochemical transformations with excitation-wavelength-dependent quantum yields of 0.3−1.0 mol/Einstein. Mass spectroscopic studies of the product solutions demonstrate the formation of S_8, presumably from the decomposition of NS. The quantitative photochemical behaviors of **1** and the nitrosyl analog **2** are compared.

Introduction

The simple diatomic molecule nitrogen monosulfide (NS) has been identified in outer space, and its gas phase chemistry has been explored.[1] In contrast, its solution phase chemistry is largely limited to a relatively small number of transition metal thionitrosyl complexes[2] $ML_n(NS)^{m+}$, and the reactions of free NS in solution are unexplored. Since analogous metal nitrosyl complexes are often quite photoactive toward the labilization of nitric oxide (NO, aka nitrogen monoxide), photolabilization from a thionitrosyl complex is a potential entry into studying the solution chemistry of this diatomic radical. Notably, while the photochemical reactions of nitrosyl complexes of the type $ML_n(NO)^{m+}$ have been extensively investigated,[3,4] to our knowledge, the quantitative photochemistry of an analogous $ML_n(NS)^{m+}$ species has never been documented. More importantly, flash photolysis of such thionitrosyl complexes would provide the rare opportunity to investigate the reaction dynamics of NS in solution, which also to our knowledge is undocumented. In this context, we report that laser flash photolysis of the thionitrosyl complex $[Cr(CH_3CN)_5(NS)](PF_6)_2$[5,6] in acetonitrile solution leads to reversible NS release, and we describe several solution phase reactions of NS. Related flash photolysis studies of the analogous nitrosyl species $[Cr(CH_3CN)_5(NO)](PF_6)_2$[7,8] are also described.

* Authors to whom correspondence should be addressed. E-mail: ford@chem.ucsb.edu (P.C.F.), dossing@kiku.dk (A.D.).
† University of Copenhagen.
‡ University of California, Santa Barbara.

(1) (a) Canaves, M. V.; de Almeida, A. A.; Boice, D. C.; Sanzovo, G. C. *Adv. Space Res.* **2007**, *39*, 451–457. (b) Blitz, M. A.; McKee, K. W.; Pilling, M. J.; Vincent, M. A.; Hillier, I. H. *J. Phys. Chem. A* **2002**, *106*, 8406–8410.
(2) Pandey, K. K. *Prog. Inorg. Chem.* **1992**, *40*, 445–502.
(3) Ford, P. C.; Lorkovic, I. M. *Chem. Rev.* **2002**, *102*, 993–1017.
(4) Ford, P. C.; Wecksler, S. *Coord. Chem. Rev.* **2005**, *249*, 1382–1395.
(5) Herberhold, M.; Haumaier, L. *Z. Naturforsch.* **1980**, *35B*, 1277–1280.
(6) Dethlefsen, J. W.; Døssing, A. *Inorg. Chim. Acta* [Online] DOI: 10.1016/j.ica.2008.02.014.
(7) Døssing, A.; Frey, A. M. *Inorg. Chim. Acta* **2006**, *359*, 1681–1684.
(8) Dethlefsen, J. W.; Døssing, A.; Kadziola, A. *Inorg. Chim. Acta* [Online] DOI: 10.1016/j.ica. 2008.08.001.

10.1021/ic8016936 CCC: $40.75
Published on Web 11/25/2008

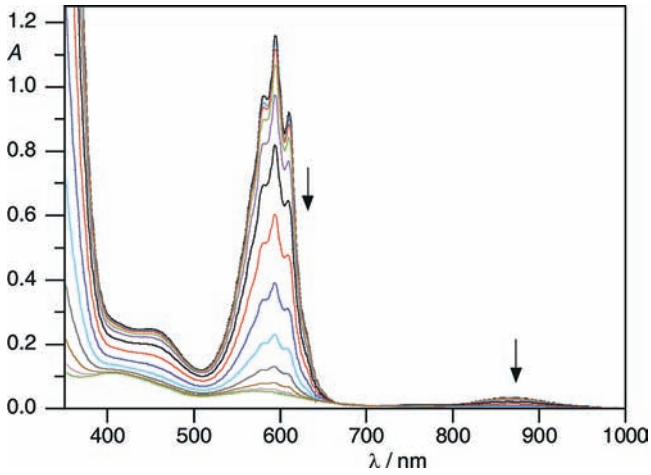

Figure 1. Changes in the optical absorption spectra following the thermal decomposition of $Cr(CH_3CN)_5(NS)^{2+}$ in aerated acetonitrile solution at ambient temperatures. The spectra were recorded every 1 h for a period of 12 h.

Results and Discussion

Qualitative Observations on the Stability of $Cr(CH_3CN)_5(NS)^{2+}$ (1) and $Cr(CH_3CN)_5(NO)^{2+}$ (2) in Acetonitrile. The dark reaction stabilities of the PF_6^- salts of **1** and **2** in acetonitrile solution were investigated. Deaerated solutions of nitrosyl complex **2** were stable and displayed no changes in the electronic spectra when kept in the dark for a period of hours. This was also true when excess $[Cr(CH_3CN)_6](BF_4)_2$ was added, which is notable given that the pentaaquochromium nitrosyl ion $Cr(H_2O)_5(NO)^{2+}$ is reported to decompose in deaerated aqueous solutions in the presence of added Cr^{2+}.[9] The addition of water or dilute sulfuric acid to acetonitrile solutions of **2** leads to the formation of $Cr(H_2O)_5(NO)^{2+}$.[7] Lastly, oxygenated acetonitrile solutions of **2** appear indefinitely stable when kept in the dark but decompose when irradiated with visible or UV light.

Deaerated acetonitrile solutions of **1** also proved to be indefinitely stable when kept in the dark. The addition of water to the acetonitrile solution (1/1, v/v) gives the complex $Cr(H_2O)_5(NS)^{2+}$ with $t_{1/2} \approx 4$ min,[6] whereas the addition of dilute sulfuric acid (2 M, H_2SO_4/MeCN, 1/10, v/v) leads to decomposition within 5 min. The addition of $[Cr(CH_3CN)_4](BF_4)_2$ leads to a very slow decomposition. The latter observation may be attributed to acetic acid impurities in this material, which was synthesized from chromium(II) acetate.[10] Aerated ($p_{O_2} = 0.20$ bar) acetonitrile solutions of **1** are not stable even in the dark (see Figure 1), and the decomposition appears to be autocatalytic. Total decomposition takes approximately 12 h, independent of the starting concentration of the $Cr(CH_3CN)_5(NS)^{2+}$ salt.

Continuous photolysis of deaerated acetonitrile solutions of **1** using 366 nm light from a 200 W Hg lamp leads to very little net photochemistry, whereas irradiation with a pulsed laser (355 nm) leads to much faster decomposition

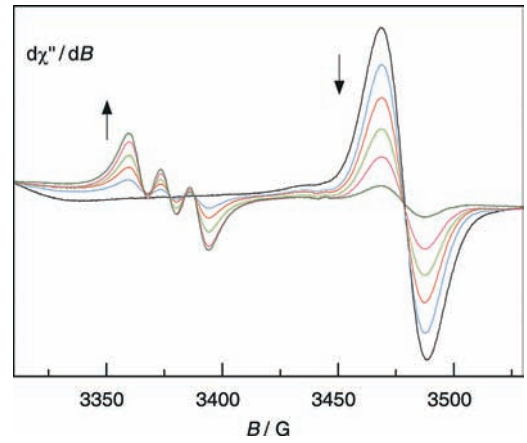

Figure 2. EPR spectra of a solution containing 13 mM $[Cr(CH_3CN)_5(NS)](PF_6)_2$ and 50 mM $[Fe(S_2NCEt_2)_2]$ in deoxygenated $MeCN/CH_2Cl_2$ (1:7 v/v). The first spectrum was before exposure to light, whereas the following spectra were taking during photolysis of the solution.

(see below). Aerated solutions are quite photosensitive. The qualitative response of acetonitrile solutions of **1** to photoexcitation suggests that NS is labilized reversibly from this cation (eq 1) in accord with previous observations of NO release from **2** and related complexes. The net photochemistry in aerated solution can be attributed to the trapping of one or both of the photoproducts (NS or $Cr(CH_3CN)_6^{2+}$) by dioxygen.

$$\underset{(\mathbf{1})}{Cr(CH_3CN)_5(NS)^{2+}} + CH_3CN \underset{}{\overset{h\nu}{\rightleftharpoons}} \underset{(\mathbf{3})}{Cr(CH_3CN)_6^{2+}} + NS \qquad (1)$$

Photoinduced NS Transfer from Chromium to Iron. In the case of the nitrosyl complex, it was recently demonstrated[8] that photolysis of a deoxygenated acetonitrile solution of **2** in the presence of the well-known spin-trapping agent $Fe(S_2CNEt_2)_2$[11] resulted in NO transfer to the iron center. This was shown by electron paramagnetic resonance (EPR) spectroscopy, which demonstrated the appearance of the characteristic spectrum of $Fe(S_2CNEt_2)_2(NO)$ ($S = 1/2$) upon photolysis. The advantage of using $Fe(S_2CNEt_2)_2$ ($S = 2$)[12] as a trapping agent is that it is X-band EPR-silent in solution, as is the other photolysis product, **3** ($S = 2$).

The EPR spectrum recorded for a solution of **1** plus $Fe(S_2CNEt_2)_2$ before the photolysis is that of $Cr(CH_3CN)_5(NS)^{2+}$ ($S = 1/2$), which consists of a broad band located at $g = 1.98$, owing to the superhyperfine coupling to ^{14}N ($I = 1$) in the five acetonitrile ligands. During photolysis with all lines from a Hg lamp, new bands grew in, presumably as the result of the formation of $Fe(S_2CNEt_2)_2(NS)$ ($S = 1/2$; eq 2), whereas the broad band from **1** disappears (Figure 2).

$$(Cr(CH_3CN)_5(NS)^{2+} + Fe(S_2CNEt_2) + CH_3CN \xrightarrow{h\nu}$$

$$Cr(CH_3CN)_6^{2+} + Fe(S_2CNEt_2)_2(NS) \quad (2)$$

From the final spectrum, the superhyperfine coupling constant A_{iso}^N in $Fe(S_2CNEt_2)_2(NS)$ can be calculated as $A_{iso}^N = 12.2$

(9) Armor, J. N.; Buchbinder, M. *Inorg. Chem.* **1973**, *12*, 1086–1090.
(10) Henriques, R. T.; Herdtweck, E.; Kühn, F. E.; Lopes, A. D.; Mink, J.; Romão, C. C. *J. Chem. Soc., Dalton Trans.* **1998**, 1293–1297.
(11) Yoshimura, T.; Kotake, Y. *Antioxid. Redox Signal.* **2004**, *6*, 639–647.
(12) De Vries, J. L. K.; Keijzers, C. P.; De Boer, E. *Inorg. Chem.* **1972**, *11*, 1343–1347.

Table 1. Calculated and Experimental Geometrical Parameters for the Fe(NE) Complexes

compound	method	dist.(Fe−N)/Å	dist.(N−E)/Å	angle(Fe−N−E)/°	ref
$Fe(S_2CNMe_2)_2(NO)$	BP	1.665	1.178	172.90	
$Fe(S_2CNMe_2)_2(NS)$	BP	1.671	1.549	176.50	
$Fe(S_2CNMe_2)_2(NSe)$	BP	1.658	1.714	173.61	
$Fe(S_2CNMe_2)_2(NO)$	exptl[a]	1.720(5)	1.102(7)	170.4(6)	14
$Fe(S_2CNEt_2)_2(NO)$	exptl	1.69(4)	1.16(5)	174(4)	15

[a] $T = -80$ °C.

Table 2. Mulliken Spin Densities in $Fe(S_2CNMe_2)_2(NE)$ (E = O, S, Se)

Compound	Fe	N	E
$Fe(S_2CNMe_2)_2(NO)$	+1.12	−0.074	−0.077
$Fe(S_2CNMe_2)_2(NS)$	+1.26	−0.11	−0.19
$Fe(S_2CNMe_2)_2(NSe)$	+1.18	−0.11	−0.11

Table 3. Hyperfine Coupling Constants in $Fe(S_2CNMe_2)_2(NE)$ (E = ^{17}O, ^{33}S)

compound	$A_{iso}(^{57}Fe)$/MHz	$A_{iso}(^{14}N)$/MHz	$A_{iso}(E)$/MHz
$Fe(S_2CNMe_2)_2(NO)$	−10.09	+50.51	−15.62
$Fe(S_2CNMe_2)_2(NS)$	−7.97	+56.81	+17.81

$\times 10^{-4}$ cm^{-1} with $g_{iso} = 2.0400$, very close to the values that were found for $Fe(S_2CNEt_2)_2(NO)$ (12.0×10^{-4} cm^{-1} and 2.040).[13] It is somewhat surprising that the EPR parameters for $Fe(S_2CNEt_2)_2(NO)$ and $Fe(S_2CNEt_2)_2(NS)$ are so similar. The proposed[13] electronic configuration (assuming C_{2v} symmetry) suggests the following order of energy levels for the {Fe(NO)}^{7} system: $a_2(xy)^2 < b_1(xz)^2 < b_2(yz)^2 < 1a_1(z^2)^1 < 2a_1(x^2 - y^2)^0$, with the unpaired electron in the d_{z^2} orbital. Since this orbital is pointing out toward the chalcogen atom, the EPR parameters might have been expected to be more sensitive to the nature of this. No calculations seem to have been performed on this system, so we decided to compare the compounds $Fe(S_2CNMe_2)_2(NE)$ (E = O, S, and Se) by means of density-functional theory DFT calculations.

Electronic Structure of $Fe(S_2CNMe_2)_2(NE)$ (E = O, S, and Se). The relevant optimized, geometrical parameters are compiled in Table 1. All three complexes contain an essentially linear Fe−N−E core with Fe−N distances that are identical within 0.01 Å. Within the experimental errors, $Fe(S_2CNEt_2)_2(NO)$ and $Fe(S_2CNMe_2)_2(NO)$ have almost identical geometrical parameters for the Fe(NO) core. Hence, the methyl complexes were chosen as model systems. The calculated geometrical parameters for $Fe(S_2CNMe_2)_2(NO)$ fit the experimental values well, while the values for $Fe(S_2CNMe_2)_2(NS)$ lie within the values for other characterized thionitrosyl complexes.[2] Since only one selenonitrosyl has been characterized by means of X-ray diffraction,[16] it is unreasonable to make any comparison. Molecular orbital calculations employing the PM3 model on the complexes $(C_5H_5)Cr(CO)_2(NE)$ (E = O, S, Se, Te) showed a slight decrease from 1.674 to 1.642 Å in Cr−N bond distances when going from oxygen to tellurium.[17] This confirms the independence of our Fe−N distances from the nature of the chalcogen atom. The Mulliken spin densities within the Fe(NE) core are compiled in Table 2. Interestingly, the large, positive spin density on the iron atom and the small, negative spin densities on the nitrogen and chalcogen atoms are essentially independent of the nature of the chalcogen atom. The hyperfine coupling constants to ^{57}Fe, ^{14}N, ^{17}O, and ^{33}S have been calculated for the nitrosyl and thionitrosyl complexes and are compiled in Table 3. The hyperfine coupling constants to ^{57}Fe and ^{14}N in $Fe(S_2CNEt_2)_2(NO)$ were determined experimentally without sign by Raynor et al.[13] to be $A_{iso}(^{57}Fe) = 8.6$ G $= 8.2 \times 10^{-4}$ $cm^{-1} = 24.5$ MHz and $A_{iso}(^{14}N) = 12.6$ G $= 12.0 \times 10^{-4}$ $cm^{-1} = 35.9$ MHz. We note that our calculated $A_{iso}(^{57}Fe)$ is approximately 60% too low, whereas our calculated $A_{iso}(^{14}N)$ is 40% too high. It is, however, a common observation that hyperfine coupling constants are difficult to calculate with greater accuracy. The calculated values are found to be dependent on the nature of the chalcogen atom. The experimental difference between the values of A for the two complexes in Table 3 is, however, smaller than the difference between the calculated and experimental value for the nitrosyl complex, indicating that the calculations are not sufficiently accurate.

For each complex, there are seven pairs of spin orbitals with 3d metal and π^*(NE) character stemming from interactions between the five 3d orbitals on the iron atom and the two π^* orbitals on the NE ligand. From orbital energies in Supporting Information Tables S-1 and S-2, the orbital diagrams in Figure 3, and contour plots of the spin orbitals (Supporting Information Figure S1), it is evident that the orders of the populated orbitals in the nitrosyl and thionitrosyl complexes are almost identical, and in both cases, the highest occupied molecular orbital (HOMO) has d_{z^2} character. Furthermore, the electron density within the Fe(NE) core is almost independent of the nature of the chalcogen atom. The orbital diagram in Figure 3 demonstrates the following three conditions. First, the order of the spin orbitals in the nitrosyl and thionitrosyl complexes are not identical, but the orbitals which are not appearing in the same order are lying close to each other. Second, the HOMO is the $1a_1(d_{z^2})$ orbital. Third, the energy differences between the $2b_2$ and $1b_2$ and the $2b_1$ and $1b_1$ orbitals are smaller in the thionitrosyl complex than in the nitrosyl complex (see Supporting Information Table S-2). This indicates that NS is a weaker π-acceptor than NO.

On the basis of the DFT calculations, we conclude that very similar hyperfine coupling constants for the nitrogen atoms in $Fe(S_2CNEt_2)_2(NO)$ and $Fe(S_2CNEt_2)_2(NS)$ are

(13) Goodman, B. A.; Raynor, J. B.; Symons, M. C. R. *J. Chem. Soc. A* **1969**, 2572–2575.
(14) Davies, G. R.; Jarvis, J. A. J.; Kilbourn, B. T.; Mais, R. H. B.; Owston, P. G. *J. Chem. Soc. A* **1970**, 1275–1283.
(15) Colapietro, M.; Domenicano, A.; Scaramuzza, L.; Vaciago, A.; Zambonelli, L. *Chem. Commun.* **1967**, 583–584.
(16) Crevier, T. J.; Lovell, S.; Mayer, J. M.; Rheingold, A. L.; Guzei, I. A. *J. Am. Chem. Soc.* **1998**, *120*, 6607–6608.
(17) Teague, C. M.; O'Brien, T. A.; O'Brien, J. F. *J. Coord. Chem.* **2002**, *55*, 627–631.

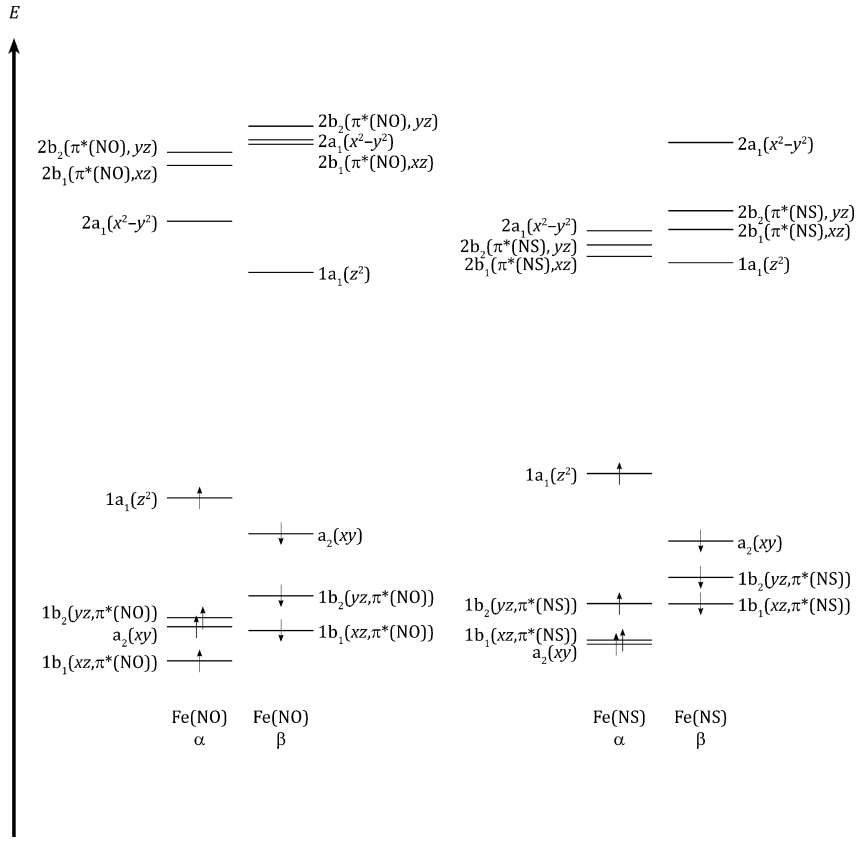

Figure 3. Schematic view of the energies of the spin orbitals in the complexes $Fe(S_2CNMe_2)_2(NO)$ and $Fe(S_2CNMe_2)_2(NS)$.

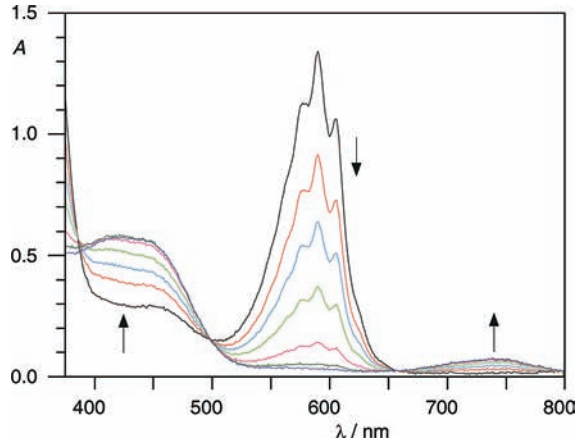

Figure 4. Optical absorption spectra changes following the white light photolysis (all lines from a mercury lamp) of a deaerated acetonitrile solution of $[Cr(CH_3CN)_5(NS)](PF_6)_2$ in the presence of NO (1 bar). The increasing absorbance bands represent the formation of $Cr(CH_3CN)_5(NO)^{2+}$.

reasonable and that the earlier assignment of the d_{z^2} orbital as the HOMO is in agreement with the computations reported here.

Photolysis-Induced Exchange of Coordinated NS with NO. In addition to trapping the released NS as illustrated above, it should be possible to trap the assumed product $Cr(CH_3CN)_6^{2+}$. This was demonstrated by carrying out the photolysis of **1** under a nitric oxide atmosphere (p_{NO} = 1 bar) in deaerated acetonitrile solution. The solution with added NO was not thermally stable, but the reaction was very slow ($t_{1/2} \approx 14$ h), so that over the time frame of the photolysis experiment, there was little dark reaction. However, upon photolysis with all lines from a Hg lamp, **1** was transformed quantitatively to **2**, indicating the photoinduced replacement of NS by NO, as indicated by eq 3 (Figure 4). The final absorption spectrum in Figure 4 is identical to the earlier published spectrum of **2**.[7] This can be taken as evidence for the formation of **3** by NS photodissociation from **1** (eq 1), since the chromium species that might accompany dissociation of NS^+, NS^-, or atomic sulfur would not be expected to react with NO to form **2**. The eventual fate of the NS formed under these circumstances is unknown. In earlier gas-phase studies, no reaction between NO and NS was observed.[1b] It is notable that the slow thermal reaction noted above gave spectral changes different from those seen for the photoinduced NS/NO exchange, but this reaction has not yet been studied in greater detail.

$$Cr(CH_3CN)_5(NS)^{2+} + NO \xrightarrow{h\nu} Cr(CH_3CN)_5(NO)^{2+} + NS \quad (3)$$

Photoinduced Decomposition of $Cr(CH_3CN)_5(NS)^{2+}$ in Solution. The quantum yield Φ_d for the photodecomposition of **1** is defined in terms of moles of $Cr(CH_3CN)_5(NS)^{2+}$ that are depleted relative to the Einsteins of light absorbed. Under the relative low intensity of the light absorbed under continuous photolysis at 366 nm in deaerated acetonitrile, the photoreaction was nearly indiscernible, and an upper limit for Φ_d of $\sim$ 0.002 mol/Einstein can be estimated. However, when the photoreaction was probed using the third harmonic (355 nm) of a pulsed (10 Hz) YAG laser as the excitation source, photoinduced decay of the absorbances due to **1** were certainly observable. The results of the quantum yields

measured under these conditions using different excitation intensities and different concentrations of added $Cr(CH_3CN)_6^{2+}$ (Supporting Information Table S-3) suggested the following trends. First, in the absence of added **3**, changing the excitation laser intensity about 5-fold had little or no effect on the quantum yield for the disappearance of **1** ($\Phi_d = 0.018 \pm 0.002$) in the absence of added **3**. Second, the addition of $[Cr(CH_3CN)_4](BF_4)_2$ (2.4−12 mM) to the solution leads to a significant decrease (3- to 5-fold) in the overall quantum yield. Although, qualitatively, higher concentrations of **3** and lower pulse intensities tended to decrease Φ_d, the scatter in the data precluded a more quantitative interpretation.

These observations are qualitatively consistent with the photoreaction shown in eq 1. The back reaction (eq 4), studied quantitatively below, is the principal fate of the reactive products $Cr(CH_3CN)_6^{2+}$ and NS.

$$Cr(CH_3CN)_6^{2+} + NS \xrightarrow{k_{on}} Cr(CH_3CN)_5(NS)^{2+} + CH_3CN \quad (4)$$

Subsequent to the excitation stimulated release of NS, the species present in scrupulously deaerated solution are **1**, **3**, and NS plus the counteranions BF_4^- and PF_6^- and the solvent itself. Although the reaction between NS and $Cr(CH_3CN)_5(NS)^{2+}$ or one of the other solution components cannot be ruled out entirely, it is likely that the pathway leading to net photoreaction is the dimerization (and subsequent oligomerization) of NS (eq 5).

$$2NS \xrightarrow{k_d} (NS)_2 \rightarrow ? \quad (5)$$

The latter can explain the observation of more photodecomposition under laser excitation where much higher initial concentrations of NS are formed in a relatively small volume. In the absence of excess Cr^{2+}, the concentrations of NS and Cr^{2+} immediately after irradiation would be identical, and the initial proportionation between the amount of NS reacting with Cr^{2+} or with another NS molecule is consequently independent of the amount of released NS. In the presence of excess Cr^{2+}, the dimerization of NS would be suppressed by enhanced back reaction but should be sensitive to increases in intensity. This is qualitatively what was observed.

A key observation supporting some oligomerization pathway for photogenerated NS is drawn from the positive ion mass spectra (EI) of irradiated and nonirradiated acetonitrile solutions of **1** which had been exposed to air before analysis. The peaks seen in irradiated solutions that were not common to both solutions had *m*/*z* values of 256 (S_8^+), 224 (S_7^+), 192 (S_6^+), 160 (S_5^+), 128 (S_4^+), 96 (S_3^+), and 64 (S_2^+), all of which would be characteristic of S_8. In addition, there were peaks at 200 (unknown), 172 (unknown), 127 (SF_5^+), and 108 (SF_4^+). It is evident that $(SN)_x$ oligomers were not present. Calculations[18] show that all isomers of S_2N_2 are unstable with respect to dissociation to N_2 and S_2. The highly reactive S_2 will ultimately end as S_8, but it is very likely that some of it might react with other species present in the solution, perhaps even to extract fluorine from the PF_6^- anion. Thus, it appears that if the SN in solution dimerizes, the species formed undergo decay to N_2 and S_2 rather than forming the more stable oligomers that should have been detected in the mass spectrum.

(18) Mawhinney, R. C.; Goddard, J. D. *Inorg. Chem.* **2003**, *42*, 6323–6337.

Table 4. Quantum Yields for the Photodecomposition of **1** in Aerated Solution

λ_{ex} (nm)	Φ_d (mol/Einstein)
366	0.31 ± 0.05
405	0.29 ± 0.10
436	0.67 ± 0.09
546	0.96 ± 0.2
580	1.04 ± 0.10

Quantum Yields for the Photolysis of 1 in Aerated Solutions. The Φ_d values were determined at the excitation wavelengths 366, 405, 436, 546, and 580 nm and are summarized in Table 4. These are dramatically higher than measured in deaerated media, presumably owing to the trapping of **1** by O_2, since NS does not react with O_2, at least in the gas phase.[1b] However, the products were not characterized. The other key feature of these data is that the quantum yield appears to be noticeably higher at longer wavelengths corresponding to the absorption band (λ_{max} = 580 nm) in which an electron is promoted from a Cr−N(S) π orbital to a Cr−N(S) π^* orbital.[7] This weakens the Cr−NS bond in agreement with the observed high value of Φ_d.

Flash Photolysis of $Cr(CH_3CN)_5(NO)^{2+}$ and $Cr(CH_3CN)_5(NS)^{2+}$. In principle, a solution of a (thio)nitrosyl complex of the type $Cr(CH_3CN)_5(NE)^{2+}$ (E = S or O) exists in the equilibrium shown in eq 6, where the *K* for formation of the NE complex equals k_{on}/k_{off}.

$$Cr(CH_3CN)_5(NE)^{2+} + CH_3CN \underset{k_{on}}{\overset{h\nu,\ k_{off}}{\rightleftharpoons}} Cr(CH_3CN)_6^{2+} + NE \quad (6)$$

The system can be disrupted by pulsed photoexcitation to give a nonequilibrium state which relaxes back to the original state. In the presence of excess **3** ([**3**] ≫ [NE]), the relaxation dynamics for this model would be exponential with the observed rate constant $k_{obs} = k_{off} + k_{on}[\mathbf{3}]$, assuming that there are no other significant decay pathways.

Such flash photolysis experiments were carried out for deoxygenated acetonitrile solutions of both $Cr(CH_3CN)_5(NO)^{2+}$ and $Cr(CH_3CN)_5(NS)^{2+}$ in the presence of excess $Cr(CH_3CN)_6^{2+}$ at different concentrations. The relaxation back to the equilibrium state as followed by time-resolved optical spectroscopy using various observation wavelengths was exponential in each case to give the pseudo-first-order rate constants k_{obs}. It is notable, however, that although regeneration of the nitrosyl complex **2** was complete, the back-reaction between NS and $Cr(CH_3CN)_6^{2+}$ was not, displaying a small degree of net photochemistry, as noted above (Supporting Information Figures S-2 and S-3). Nonetheless, the point-by-point transient spectrum recorded immediately following the flash photolysis of **1** corresponded

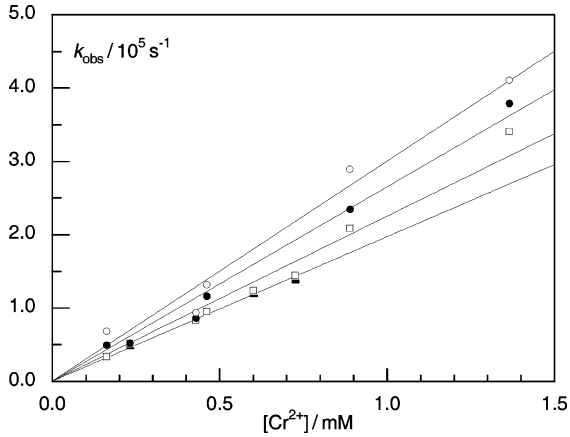

Figure 5. Plot of k_{obs} versus $[Cr^{2+}]$ for the reaction between NS and $Cr(CH_3CN)_6^{2+}$ in deaerated acetonitrile solution at 288 (■), 298 (□), 308 (•), and 318 K (○).

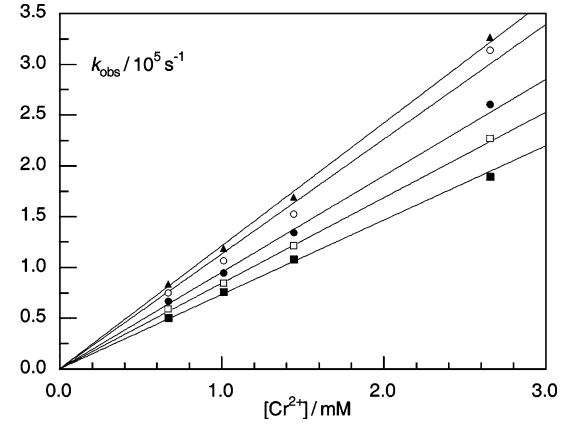

Figure 6. Plot of k_{obs} versus $[Cr^{2+}]$ for the reaction between NO and $Cr(CH_3CN)_6^{2+}$ in deaerated acetonitrile solution at 298 (■), 308 (□), 318 (•), 328 K (○), 338 K (▲).

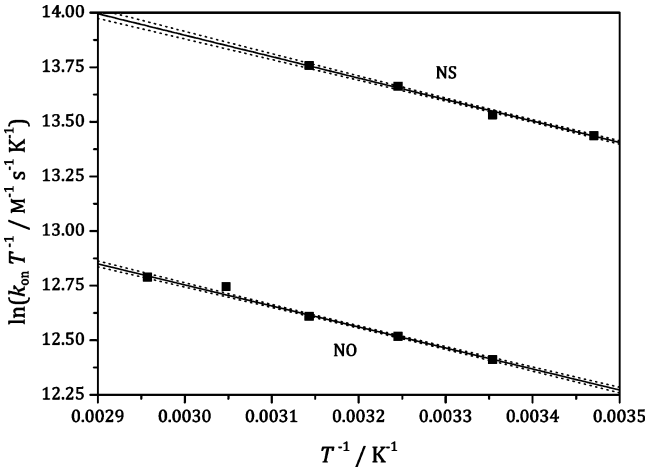

Figure 7. Eyring plots of k_{on} for the reaction between NS and NO and $Cr(CH_3CN)_6^{2+}$. The dashed curves are plus and minus one standard uncertainty.

to the difference between the spectra of the starting complex $Cr(CH_3CN)_5(NS)^{2+}$ and the $Cr(CH_3CN)_6^{2+}$ product.

For both complexes, plots of k_{obs} versus [**3**] were linear, with intercepts at zero (Figures 5 and 6); thus, on this time scale, the "off" reaction is too small to be detectable, as expected given the long lifetimes of the $Cr(CH_3CN)_5(NE)^{2+}$ ions, even in aerated solutions. The slopes of such plots give

Table 5. Second-Order Rate Constants for the Reaction between NE and $[Cr(CH_3CN)_6]^{2+}$ at Different Temperatures

T/K	288	298	308	318	328	338
k_{on}(NO)/10^8 M^{-1} s^{-1}		0.732(11)	0.842(5)	0.95(2)	1.13(3)	1.21(2)
k_{on}(NS)/10^8 M^{-1} s^{-1}	1.97(3)	2.25(8)	2.65(10)	3.00(11)		

the second-order rate constants for the "on" reaction, and at 298 K, the value for **1** is $k_{on}(NS) = (2.3 \pm 0.2) \times 10^8$ M^{-1} s^{-1} and for **2** is $k_{on}(NO) = (7.3 \pm 0.4) \times 10^7$ M^{-1} s^{-1}. Although these rate constants are of similar magnitude, the reaction of NS with $Cr(CH_3CN)_6^{2+}$ is about 3 times as fast as the comparable reaction of NO, and both are several orders of magnitude less than that expected for diffusion-limited reactions. One notable difference between NS and NO is the high dipole moment of NS ($\mu = 1.83$ D)[19] with the negative end toward nitrogen, compared to the relatively nonpolar NO ($\mu = 0.16$ D).[20] The higher electron density on nitrogen in NS compared to NO and higher polarizability of NS could explain the higher reactivity of NS toward Cr^{2+}. Analogous kinetics studies were carried out over the temperature range of 288−318 K for **1** and 298−338 K for **2** (Table 5), and Eyring plots (Figure 7) of the resulting k_{on} values gave the activation parameters $\Delta H_{on}^{\ddagger} = 8.2 \pm 0.4$ kJ mol^{-1} and $\Delta S_{on}^{\ddagger} = -57.5 \pm 1.2$ J mol^{-1} K^{-1} for the reaction of **3** with NS and $\Delta H_{on}^{\ddagger} = 8.0 \pm 0.3$ kJ mol^{-1} and $\Delta S_{on}^{\ddagger} = -67.5 \pm 1.1$ J mol^{-1} K^{-1} for the reaction of **3** with NO. The values of the observed pseudo-first-order rate constants are found in Supporting Information Table S-4.

The k_{on}(NO) value for the NO reaction with $Cr(CH_3CN)_6^{2+}$ is somewhat slower than that measured previously by Bakac and co-workers[21] for the reaction of NO with $Cr(H_2O)_6^{2+}$ in aqueous solution ($k_{on} = 2.5 \times 10^8$ M^{-1} s^{-1} at 298 K). A similar k_{on} has also been measured for the reaction of $Cr(H_2O)_6^{2+}$ with O_2,[22] but activation parameters were not reported for either of these aqueous solution reactions. Notably, all of these k_{on} values also fall within the range of the second-order rate constants observed for the reaction of various organic free radicals R• with aqueous $Cr(H_2O)_6^{2+}$ (2×10^7 to 2×10^8 M^{-1} s^{-1} at 298 K).[23] These latter rates show only a weak dependence on the nature and size of R•.

To our knowledge, there have been no previous kinetics studies evaluating the reactivity of nitrogen monosulfide in solution.

From a mechanistic perspective, the reactivity of all of these species with solvated Cr^{2+} would appear to be dominated by the lability of the Cr(II) center itself, which in water exchanges its solvent ligands with first-order rate constants of $\sim 10^9$ s^{-1}.[24] This observation is consistent with the conclusion based on activation volume measurements by

(19) Byfleet, C. R.; Carrington, A.; Russel, D. K. *Mol. Phys.* **1971**, *20*, 271–277.
(20) Liu, Y.; Guo, Y.; Lin, J.; Huang, G.; Duan, C.; Li, F. *Mol. Phys.* **2001**, *99*, 1457–1461.
(21) Nemes, A.; Pestovsky, O.; Bakac, A. *J. Am. Chem. Soc.* **2002**, *124*, 421–427.
(22) Sellers, R. M.; Simic, M. G. *J. Chem. Soc., Chem. Commun.* **1975**, 401–402.
(23) van Eldik, R.; Gaede, W.; Cohen, H.; Meyerstein, D. *Inorg. Chem.* **1992**, *31*, 3695–3696.

van Eldik et al.[23] that the reactions of Cr^{2+} with the organic radicals occur by an interchange dissociative (I_d) mechanism. In this context, the low $\Delta H_{on}^{\ddagger}$ values would be consistent with a weak Cr—OH_2 bond in the hexaquo ion owing to the strong Jahn−Teller distortion of this high-spin d^4 complex. However, the negative $\Delta S_{on}^{\ddagger}$ values for both $k_{on}(NO)$ and $k_{on}(NS)$ imply that there may be considerable bond formation in the transition states of both reactions. For comparison, the k_{on} for NO reaction with $Fe(H_2O)_6^{2+}$ is reported to be 1.4×10^6 M^{-1} s^{-1} with $\Delta H_{on}^{\ddagger} = 37.1$ kJ mol^{-1} and $\Delta S_{on}^{\ddagger} = -3$ J mol^{-1} K^{-1} and again is argued on the basis of activation volume measurements ($\Delta V_{on}^{\ddagger} = +6.1$ cm^3 mol^{-1}) to occur via an I_d mechanism.[25] The faster reactions of small radicals with the Cr(II) centers than those with iron(II) would be expected given the much greater labilities of the solvated chromium(II) ions.[26]

Summary

We have reported here the first study involving the quantitative dynamics of the diatomic molecule nitrogen monosulfide in liquid solutions. The NS was generated by the flash photolysis of the thionitrosyl chromium complex ion $Cr(CH_3CN)_5(NS)^{2+}$. Not surprisingly, the reactivity of NS prepared in this manner is largely analogous to that of the electronically homologous NO radical generated in a similar fashion. The very fast back reaction of NS with $Cr(CH_3CN)_6^{2+}$ is about 3× faster than that of NO, but this reactivity is largely dominated by the lability of the solvated Cr^{2+} ion. In addition, NS can be transferred to an iron(II) center by photochemical labilization from **1** followed by trapping by $Fe(S_2CNEt_2)_2$, again in analogy to the chemistry of NO. One key difference between NS and NO under these conditions, however, is the tendency of NS to undergo oligomerization pathways, as evidenced by the irradiation intensity- (hence, NS-concentration-) dependent side reactions seen in the photochemical experiments. The tendency of NS toward such processes is understandable given the much greater stability of $(NS)_x$ oligomers versus that of the $(NO)_x$ homologues.[27]

Experimental Section

Materials. The chromium complexes $[Cr(CH_3CN)_5(NO)](PF_6)_2$,[28] $[Cr(CH_3CN)_5(NS)](PF_6)_2$,[5] and $[Cr(CH_3CN)_4](BF_4)_2$[10] were synthesized by literature methods. Acetonitrile (HPLC-grade) was purchased from EMD, distilled over CaH_2 under dinitrogen, degassed under reduced pressure, and stored in a glovebox under an atmosphere of argon.

Instrumentation. Optical absorption spectra were recorded for solutions in 1.0 cm quartz cuvettes using Hewlett-Packard 8452A diode array, Perkin-Elmer Lambda 40, and Cary 118 spectrophotometers. EPR spectra were recorded on a Bruker Elexsys E 500 instrument, operated at the X-band, equipped with a frequency counter and a Gauss-meter. The final EPR spectrum was simulated by use of a program written by Dr. H. Weihe (University of Copenhagen, 2007).[29]

Solution Preparation. Due to the water and oxygen sensitivity of key compounds, solutions were prepared and transferred to a Schlenk quartz cuvette in a glovebox under an argon atmosphere. Solutions with known concentrations of $Cr(CH_3CN)_5(NE)^{2+}$ and $Cr(CH_3CN)_6^{2+}$ were prepared gravimetrically.

Spin Trapping of NS. The photolysis of a deoxygenated MeCN/CH_2Cl_2 (1:7 v/v) solution of 13 mM **1** and 50 mM $[Fe(S_2CNEt_2)_2]$ was carried out using an EPR capillary inside a larger EPR tube sealed with a rubber septum under a nitrogen atmosphere in a glovebox. At regular intervals during the photolysis with the Hg lamp, an EPR spectrum of the solution was recorded.

NS/NO Exchange. A solution of **2** was deaerated by two freeze−pump−thaw cycles, and ∼1 bar of pure NO was added to the Schlenk cuvette. The stirred solution was irradiated with light from a Hg lamp (all lines), as described below.

Quantum Yields in Aerated Solutions. The light source for the measuring of quantum yields in the presence of oxygen was collimated light from a 200 W Hg lamp. Chemical actinometry was carried out on stirred solutions in a thermostatted ($T = 298$ K), square 1.0 cm quartz cuvette on an optical train by the use of $K_3[Fe(C_2O_4)_3]$ ($\lambda < 450$ nm)[30] and $K[Cr(NH_3)_2(NCS)_4]$ ($\lambda > 450$ nm)[31] solutions. The intensity of absorbed light was in the range $(0.3-2.4) \times 10^{-6}$ Einstein s^{-1} L^{-1}, with concentrations of **1** being 1−4 mM. The quantum yields were found by extrapolating a plot of Φ versus n to $n = 0$.

Quantum Yields in Deaerated Solutions. The light source for the measuring of quantum yields in the absence of oxygen was the third harmonic ($\lambda_{exc} = 355$ nm) of a Spectra-Physics INDI-HG Nd/YAG pulse laser. The power was measured with a Molectron Power Max 500 A laser power meter. The continuous photolysis was carried out in a square 1.0 cm quartz Schlenk cuvette placed in a cuvette holder without stirring. The volume of the solution was approximately 4 mL. The solution was manually stirred every 10 s, that is, every 100 laser pulses. The intensity of absorbed laser light was in the range 8−80 mJ/pulse ($(0.6-7.3) \times 10^{-4}$ Einstein s^{-1} L^{-1}), with concentrations of **1** being 1.8−2.5 mM. The quantum yields were found by extrapolating a plot of Φ versus n to $n = 0$.

Flash Photolysis Instrumentation. The system at UCSB for time-resolved optical spectroscopy has previously been described in detail.[32] The laser flash photolysis experiments utilized the third harmonic ($\lambda_{exc} = 355$ nm) of a Spectra-Physics INDI-HG Nd/YAG pulse laser as the excitation source. Laser power was 80 mJ/pulse for $Cr(CH_3CN)_5(NO)^{2+}$ and 30 mJ/pulse for $Cr(CH_3CN)_5(NS)]^{2+}$ solutions, with a pulse duration of 10 ns. For the experiments with **2**, the probe beam was the output from a 65 W halogen lamp perpendicular to the excitation beam; the PMT was an RCA 1P28. For those with **1**, the probe beam was the output from a 300 W xenon lamp collinear to the excitation beam; the PMT was a red-sensitive EMI 9958QA. Wavelengths were selected prior to the sample using a high-efficiency SPEX grating monochromator and reselected and focused after the sample using a high-resolution SPEX grating monochromator. The output from the PMT was recorded by a Tektronix TDS 540 digital oscilloscope and transferred to a computer for data analysis and storage.

(24) Richens, D. T. *The Chemistry of Aqua Ions*; John Wiley & Sons: New York: 1997.
(25) Wanat, A.; Schneppensieper, T.; Stochel, G.; van Eldik, R.; Bill, E.; Wieghardt, K. *Inorg. Chem.* **2002**, *41*, 4–10.
(26) Helm, L.; Merbach, A. E. *Chem. Rev.* **2005**, *105*, 1923–1959.
(27) Salahub, D. R.; Messmer, R. B. *J. Chem. Phys.* **1976**, *64*, 2039–2047.
(28) Clamp, S.; Connelly, N. G.; Taylor, G. E.; Louttit, T. S *J. Chem. Soc., Dalton Trans.* **1980**, 2162–2169.
(29) Glerup, J; Weihe, H. *Acta Chem. Scand.* **1991**, *45*, 444–448.
(30) Calvert, J. G.; Pitts, J. N., Jr. *Photochemistry*; Wiley & Sons: New York, 1966; pp 783−786.
(31) Wegner, E. E.; Adamson, A. W. *J. Am. Chem. Soc.* **1966**, *88*, 394–404.
(32) Bridgewater, J. S.; Netzel, T. L.; Schoonover, J. R.; Massick, S. M.; Ford, P. C. *Inorg. Chem.* **2001**, *40*, 1466–1476.

The Schlenk cuvette was allowed to calibrate for at least 30 min in the thermostatted cuvette holder subsequent to changing the temperature.

The observed first-order rate constant, k_{obs}, is obtained from first-order curve fitting to the $t,\Delta A$ data, with the first 1 μs being discounted due to fluorescence and scattered laser light. For **2**, the final rate constant is the average of five runs consisting of an average of 25 laser shots each; for **1**, it is the average of 10 runs consisting of an average of 250 laser shots each. The back reaction was followed for at least eight half lives.

The second-order rate constants for the "on" reaction were obtained from a least-squares fit of the equation $k_{obs} = k_{off} + k_{on}[\mathbf{3}]$ to the $[\mathbf{3}],k_{obs}$ data, forcing $k_{off} = 0$. The k_{on} values at different temperatures were used to construct linear Eyring plots, from which the activation enthalpy and entropy were determined.

DFT Calculations. The ADF (version 2006) program package has been used exclusively. In all calculations, a basis set of triple-ζ quality with two polarization functions (TZ2P) was implemented. The exchange-correlation functional consisted of a VWN5 LDA part[33] and a GGA-part of the exchange and correlation corrections by Becke[34] and Perdew,[35] respectively (commonly formulated as BP). The spin densities, EPR parameters, and orbital energies were in all cases calculated from the geometry-optimized structures. The functional of Perdew and Wang[36] (PW91) was also applied. Optimized geometries and EPR coupling constants were—for both the nitrosyl and thionitrosyl complex—found to be fairly insensitive to this change in the exchange-correlation functional. The selenonitrosyl yielded a nonaufbau solution with PW91 and has not been considered.

Acknowledgment. P.C.F. and R.D.R. thank the National Science Foundation (CHE- 0749524) for partial support of this research. J.W.D. and A.D. thank Carlsbergs Mindelegat and the The Danish Chemical Society for support of this research.

Supporting Information Available: Supporting Information (9 pp) includes tables of DFT calculations, quantum yield and kinetics data, figures showing contour plots of the spin orbitals in $Fe(S_2CNMe_2)_2(NO)$ and $Fe(S_2CNMe_2)_2(NS)$, and examples of temporal decays following flash photolysis of **1** and **2**. This material is available free of charge via the Internet at http://pubs.acs.org.

IC8016936

(33) Vosko, S. H.; Wilk, L.; Nusair, M. *Can. J. Phys.* **1980**, *58*, 1200–1211.
(34) Becke, A. D. *Phys. Rev. A: At., Mol., Opt. Phys.* **1988**, *49*, 3098–3100.
(35) Perdew, J. P. *Phys Rev. B: Condens. Matter Mater. Phys.* **1986**, *33*, 8822–8224.
(36) Perdew, J. P.; Chevary, J. A.; Vosko, S. H.; Jackson, K. A.; Pederson, M. R.; Singh, D. J.; Fiolhais, C. *Phys. Rev. B: Condens. Matter Mater. Phys.* **1992**, *46*, 6671–6687.